

Supporting information for

Frank–Kasper Phases in Charge Transfer Complexes Enable Tunable Photoelectronic Properties

Xinyue Zhao^{†a}, Chenhui Wei^{†a}, Fuzhou Wang^a, Xinran Zhang^a, Jianchuang Wang^a, Mengfei Wang^a, Maoxin Zhang^a, Chunxiu Zhang^{*a}, Erqiang Chen^{*b}, and Haifeng Yu^{*c}

^aInformation Recording Materials Lab, Beijing Key Laboratory of Printing & Packaging Materials and Technology, Beijing Institute of Graphic Communication. Beijing, 102600, China

Email: zhangchunxiu@bigc.edu.cn

^bBeijing National Laboratory for Molecular Sciences, Key Laboratory of Polymer Chemistry and Physics of Ministry of Education, Center for Soft Matter Science and Engineering, College of Chemistry and Molecular Engineering, Peking University, Beijing 100871 (China)

Email: eqchen@pku.edu.cn

^cInstitute of new structural materials, School of Materials Science and Engineering, and Key Laboratory of Polymer Chemistry and Physics of Ministry of Education, Peking University, Beijing 100871, China

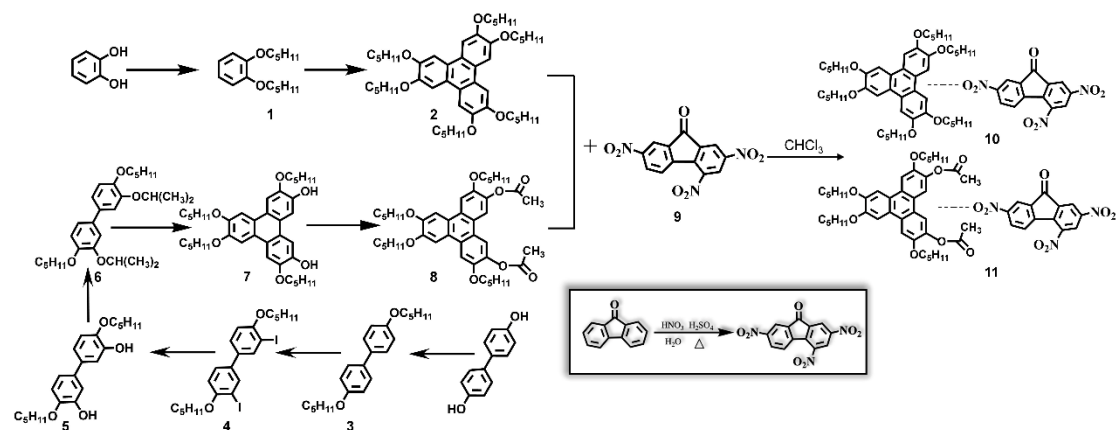
Email: yuhaifeng@pku.edu.cn

Materials. All chemicals were purchased from Aladdin and all solvents from Aldrich. All chemicals and solvents were used without further purification. Silica gel 60 (200-300 mesh ASTM) and silica gel 60 glass thin-layer chromatography were used for the purification and identification of the reaction, respectively.

Characterization. Fourier transform infrared spectroscopy (FTIR) was carried out on a Shimadzu FTIR-8400 spectrometer using KBr pellets. Raman spectra (Raman) were obtained on Renishaw in Via using a wavelength of 758 nm. Ultraviolet-visible (UV-vis) absorption spectra were measured on UV-2501 absorption spectrometer using thin film. ¹H-NMR were recorded by a Bruker NMR spectrometer (DMX 300 MHz) in CDCl₃, and chemical shifts were given as units of measurement and expressed in parts per million (δ) with tetramethylsilane (TMS) as a reference. Multiplicities of peaks are expressed as s = singlet, d = doublet, t = triplet, m = multiplet. Mass spectrometry (MS) was measured by Fourier Transform Ion Cyclotron Resonance Mass Spectrometer. The thermal properties were characterized using differential scanning calorimetry (DSC) on a Netzsch DSC 200. The first heating cycles were neglected to exclude influences of thermal history. The optical properties were characterized by a Polarizing Optical Microscope (POM) on a Leica DM4500P with a Linkam TMS94 hot stage. The LC textures were obtained during the cooling process at 10° C/min from its isotropic phase. Structural character rations of samples were characterized by 1D wide-angle X-ray diffraction (1D WAXD) through a Bruker D8 Advance diffractometer equipped with a variable temperature controller, and two-dimensional wide-angle X-ray diffraction (2DXRD) using a 40KV FL tube as the X-ray source (Cu K α). The morphologies were investigated by Transmission Electron Microscope TEM (FEI Tecnai G2 20

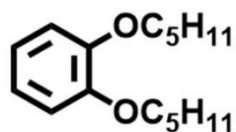
STWIN).

1. Syntheses and molecular schemes



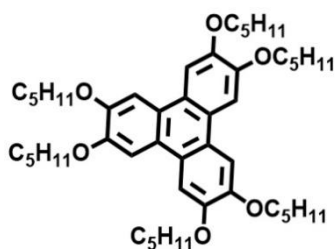
Scheme S1. Synthesis routes of Charge transfer complexes discotic liquid crystal molecule

Preparation of 1,2-bis(pentyloxy)benzene (1)



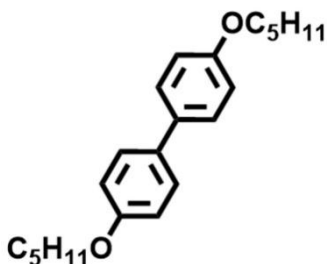
Add catechol (60g), potassium iodide (245g), and potassium carbonate (13.63g) to the acetone/ethanol mixed solution (100ml/200ml), stir for one hour, slowly add bromo-n-pentane (245g). After heating and refluxing for 24 hours, it is purified by chromatography to obtain a transparent liquid (yield 87%). $^1\text{H-NMR}$ δ (ppm) (300 MHz, CDCl_3): 6.90 (s, 4 H), 4.02-3.98 (t, 4 H), 1.88-1.79 (m, 4 H), 1.44-1.35 (m, 8 H), 0.95-0.91 (d, 6 H).

Preparation of 2,3,6,7,10,11-hexakis(pentyloxy)triphenylene (2)



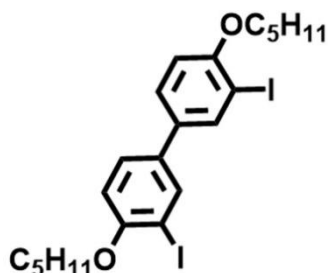
Add 1,2-bis(pentyloxy)benzene (40g) to anhydrous dichloromethane (160ml), stir mechanically for half an hour and then slowly add ferric chloride (120g). After reacting at room temperature for 3 hours, it was purified by column chromatography to obtain a white solid (yield 77%). $^1\text{H-NMR}$ δ (ppm) (300 MHz, CDCl_3): 7.83(s, 6 H), 4.25 (t, 12 H), 1.99 (t, 12 H), 1.60-1.49 (m, 24 H), 0.99 (t, 18 H).

Preparation of 4,4'-dipentoxybiphenyl (3).



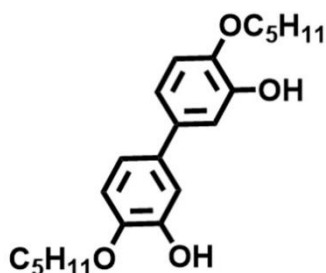
4,4'-dihydroxybiphenyl (97.8g), K_2CO_3 (240g), KI (9.7g) and hexadecyl trimethyl ammonium bromide (9.7g) were added to ethanol/acetone (300ml/100ml) solvent and the mixture was stirred under reflux. After one hour, n-pentane bromide (225.6g) was added and the compound was refluxed for another 24h. Once the reaction was complete, the product was washed in ice water, then filtered and recrystallized to obtain white scales solid (yield 97%). $^1\text{H-NMR}$ δ (ppm) (300 MHz, CDCl_3): 7.46–7.49 (d, $J = 8.7$ Hz, 4H), 6.94–6.97 (d, $J = 8.7$ Hz, 4H), 3.97–4.02 (t, $J = 6.6$ Hz, 4H), 1.77–1.86 (m, 4H), 1.35–1.52 (m, 8H), 0.93–0.97 (t, 6H).

Preparation of 3,3'-diiodo-4,4'-dipentyloxybiphenylene (4).



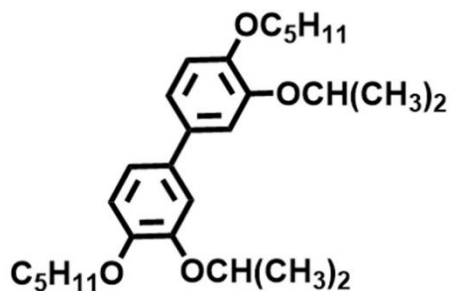
The deionized water (30ml), trichloromethane (70ml), glacial acetic acid (100g), iodine(21g), iodic acid (8.87g) and 4,4'-dipentyloxybiphenylene (32.6) were mixed by stirring. Then the concentrated sulfuric acid (3.8g) was added and the mixture was heated with stirring at 85°C for 24h. When the reaction was complete, chloroform (140ml) and deionized water (60ml) were mixed into the reactant and magnetically stirred for 10 min. The organic layer was extracted twice with saturated Na₂SO₃ solution and washed with deionized water. After that, the organic layer was dried by sodium carbonate, filtered, evaporated, vacuum dried, and recrystallized to produce white crystals (yield 94.6%). ¹H-NMR δ (ppm) (300 MHz, CDCl₃): 7.93 (d, 2H), 7.41–7.44 (d, 2H), 6.82–6.84 (d, 2H), 4.02–4.06 (t, 4H), 1.82–1.91 (m, 4H), 1.36–1.55 (m, 8H), 0.94–0.99 (t, 6H).

Preparation of 3,3'-dihydroxy-4,4'-dipentyloxybiphenylene (5).



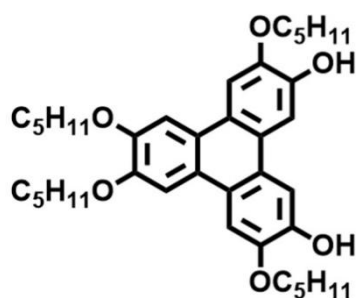
PEG-400 (240ml), deionized water (60ml), KOH (130g) and 3, 3'-diiodine-4,4'-dipentyloxybiphenylene (28.9g) were mixed and stirred for 30 min and then CuI (9g) was added carefully. The mixture was heated to 140°C with nitrogen protection. The heating was stopped after 36 h, and the reactants were acidified with hydrochloric acid when the temperature fell to room temperature. After 36 hours, the reactants were cooled to room temperature and hydrochloric acid (1mol/L) was added to acidify the solution (PH=2). After that, the solution was extracted several times with ethyl acetate, followed by rotary evaporation drying, vacuum drying, column chromatography successively, and recrystallization to obtain white needle crystal (yield 50%).¹H-NMR δ (ppm) (300 MHz, CDCl₃): 7.15 (s, 2H), 7.01– 7.04 (d, 2H), 6.87– 6.89 (d, 2H), 5.68 (s, 2H), 4.05–4.10 (t, 4H), 1.80–1.87(m, 4H), 1.37–1.45 (m, 8H), 0.93– 0.98 (t, 6H).

Preparation of 3,3'-diisopropyl-4,4'-dipentyloxybiphenylene (6).



3,3'-dihydroxy-4,4'-dipentyloxybiphenylene (6g), K_2CO_3 (13.5g), KI (1.08g) and cetyltrimethylammonium bromide were added to ethanol/acetone (75ml/75ml) solvent. Then the mixture was heated to 65 °C with nitrogen protection for 24 h. When the reaction was complete, the product was successively filtered, cyclically steamed, dried, column chromatography and recrystallized to obtain a white scaly solid (yield 80%). 1H -NMR δ (ppm) (300 MHz, $CDCl_3$): 7.10–7.12 (d, 4H), 6.92–6.95 (d, 2H), 4.49–4.57 (m, 2H), 4.00–4.05 (t, 4H), 1.80–1.89 (m, 4H), 1.42–1.53 (m, 20H), 0.93–0.97 (t, 6H).

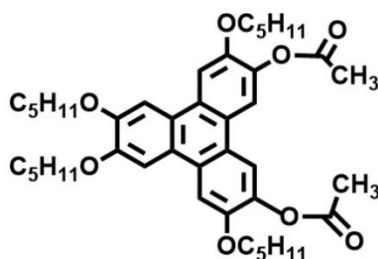
Preparation of 3,6-dihydroxy-2,7,10,11-tetrapentyloxytriphenylene (7).



3,3'-diisopropyl-4,4'-dipentyloxybenzene (13.3g), 1,2-dipentyloxybenzene (11.3g) and dichloromethane (160ml) were mixed and stirred under nitrogen protection. After 30 min, anhydrous ferric chloride was added slowly and reacted at room temperature for 12-24 hours. When the reaction was complete, the reactants were poured into 150 ml

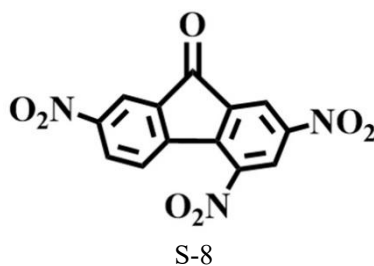
cool methanol carefully. The mixture was concentrated at room temperature and filtered. The filter cake was purified by columnar chromatography (silica, CH₂Cl₂/ Ethyl acetate (80:1) to give the final white product (yield 60%). ¹H-NMR δ (ppm) (300 MHz, CDCl₃): 7.94 (s, 2H), 7.81(s, 2H), 7.76 (s, 2H), 5.86 (s, 2H), 4.21–4.30 (t, 8H), 1.91–1.98 (m, 8H), 1.43–1.59 (m, 16H), 0.96–1.00 (t, 12H).

Preparation of 3,6-diacetoxy-2,7,10,11-tetrapentyloxytriphenylene (8).



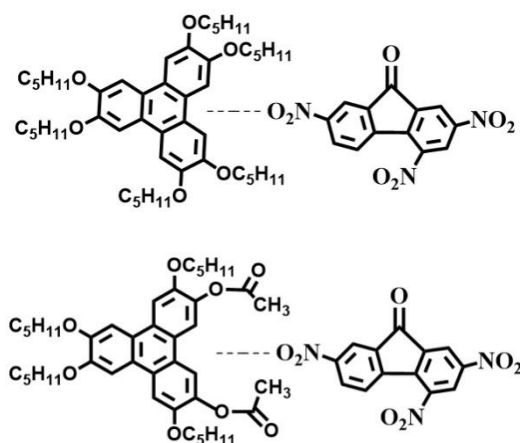
3,6-dihydroxy-2,7,10,11-tetrapentyloxytriphenylene (0.5g), dichloromethane(30ml), glacial acetic acid(0.5ml) and DMAP (18.28) were mixed under nitrogen protection and stirred at 40 °C for reflux. After 10-15 min, DCC was added and reacted for 24 hours. When the reaction was complete, the compound was processed by column chromatography and recrystallization to obtain the target product (yield 65%). ¹H-NMR δ (ppm) (300 MHz, CDCl₃): 8.03(s, 2H), 7.84 (s, 4H), 4.22 (m, 8H), 2.39 (m, 6H), 1.911(m, 8H), 1.49 (m, 16H), 1.00 (t, 12H).

Preparation of 2,4,7-trinitro-9-fluorenone (9).



Deionized water(20ml), 9-fluorenone(18g) are mixed and stirred and heated to 80 °C, then a mixture of concentrated sulfuric acid and concentrated nitric acid is added drop by drop (made by mixing concentrated sulfuric acid with the mass fraction of 96% and concentrated nitric acid with the mass fraction of 95% in accordance by the volume ratio of 1:1). After the dripping, a reflux reaction was conducted for 2h and heating was stopped. Then the reactants were cooled to room temperature and quenched by the reaction by adding 200ml water to them. After that, the reactants were successively washed by drainage, dried, and recrystallized to obtain the yellow solid (yield 85%).¹H-NMR δ (ppm) (300 MHz, CDCl₃): 9.04(s, 1H), 8.84(s, 1H), 8.68(s, 1H), 8.57(d, 1H), 8.39(d, 1H).

Synthesis of CT complexes (10,11).



The CT complexes were prepared by mixing the saturated solution of 2,3,6,7,10,11-hexakis(pentyloxy) triphenylene and 3,6-diacetyl-2,7,10,11-tetrapentyloxytriphenylene with saturated of 2,4,7-trinitro-9-fluorenone in CHCl₃. After the saturated solutions of the two compounds were mixed with TNF, the colors of the solutions changed to black and red, respectively. After a while, black and red

precipitates separate. The precipitate was filtered off and washed several times with small amounts of CHCl_3 .

2. FT-IR spectroscopy, Raman spectroscopy, ^1H NMR and MALDI-TOF mass spectrometry

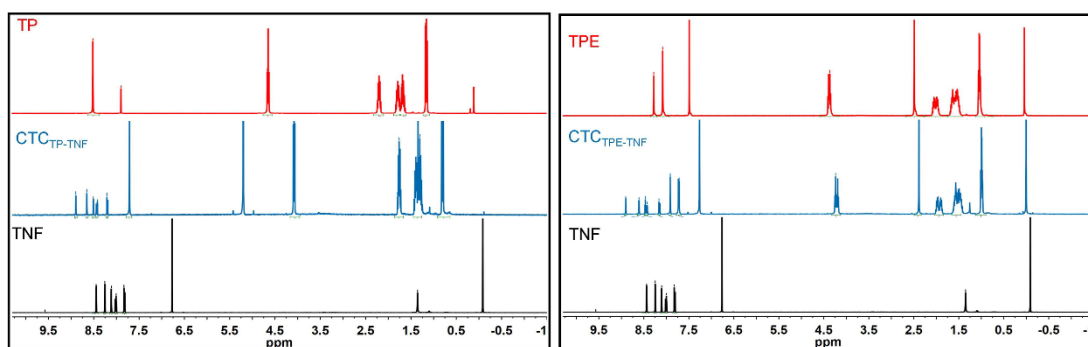


Figure S1. ^1H -NMR spectrum of CT complexes

Table S1. Summary of ^1H -NMR chemical shifts of $\text{CTC}_{\text{TP-TNF}}$.

Sample	PPm					
	1	2	3	4	5	6
TP	7.84	4.25	1.99	1.60	1.49	0.99
$\text{CTC}_{\text{TP-TNF}}$	7.72	4.14	1.85	-	1.39	0.88

Table S2. Summary of ^1H -NMR chemical shifts of $\text{CTC}_{\text{TPE-TNF}}$.

Sample	PPm						
	1	2	3	4	5	6	7
TPE	8.03	7.84	4.22	2.38	1.91	1.49	1.00
$\text{CTC}_{\text{TPE-TNF}}$	7.91	7.71	4.24	2.38	1.95	1.53	0.97

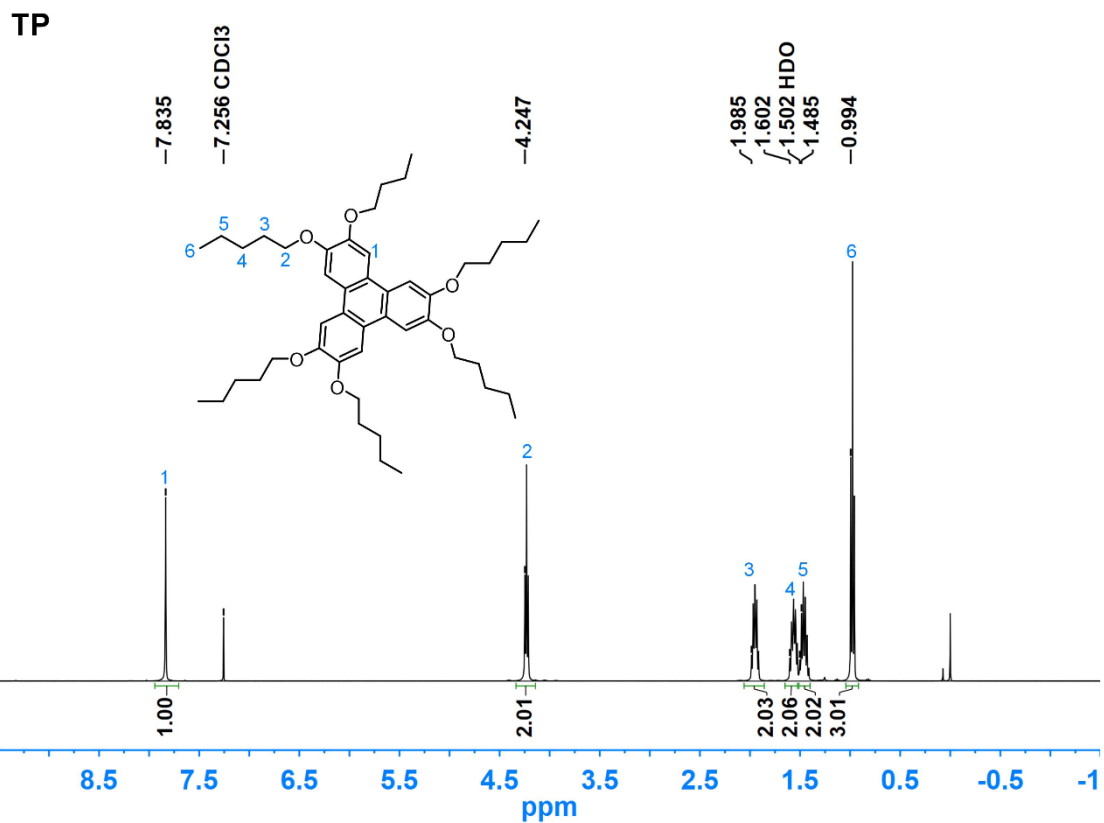


Figure S2. $^1\text{H-NMR}$ spectrum of compound TP

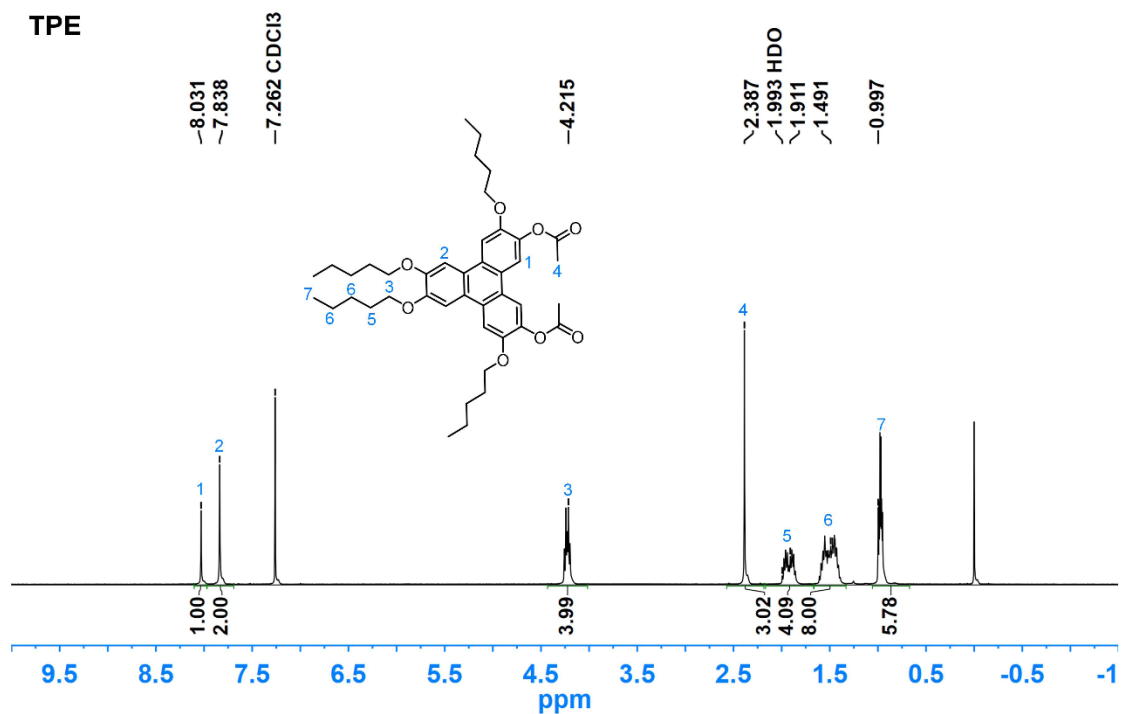


Figure S3. $^1\text{H-NMR}$ spectrum of compound TPE

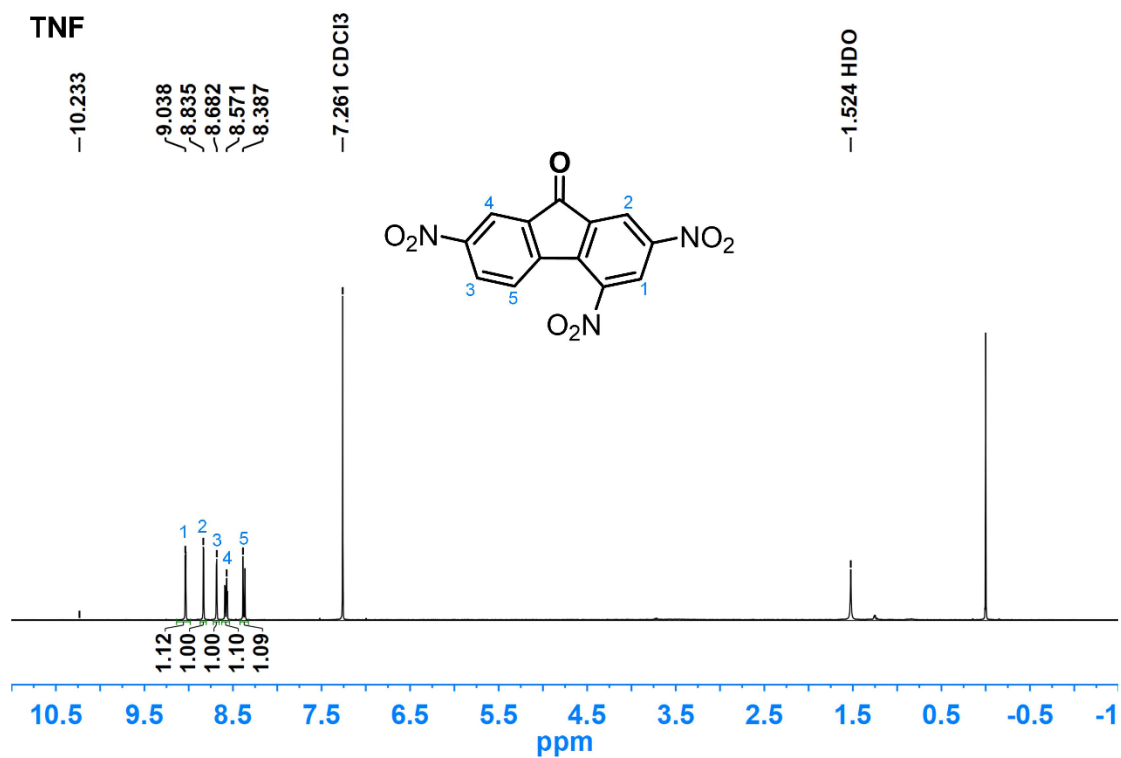


Figure S4. ¹H-NMR spectrum of compound TNF

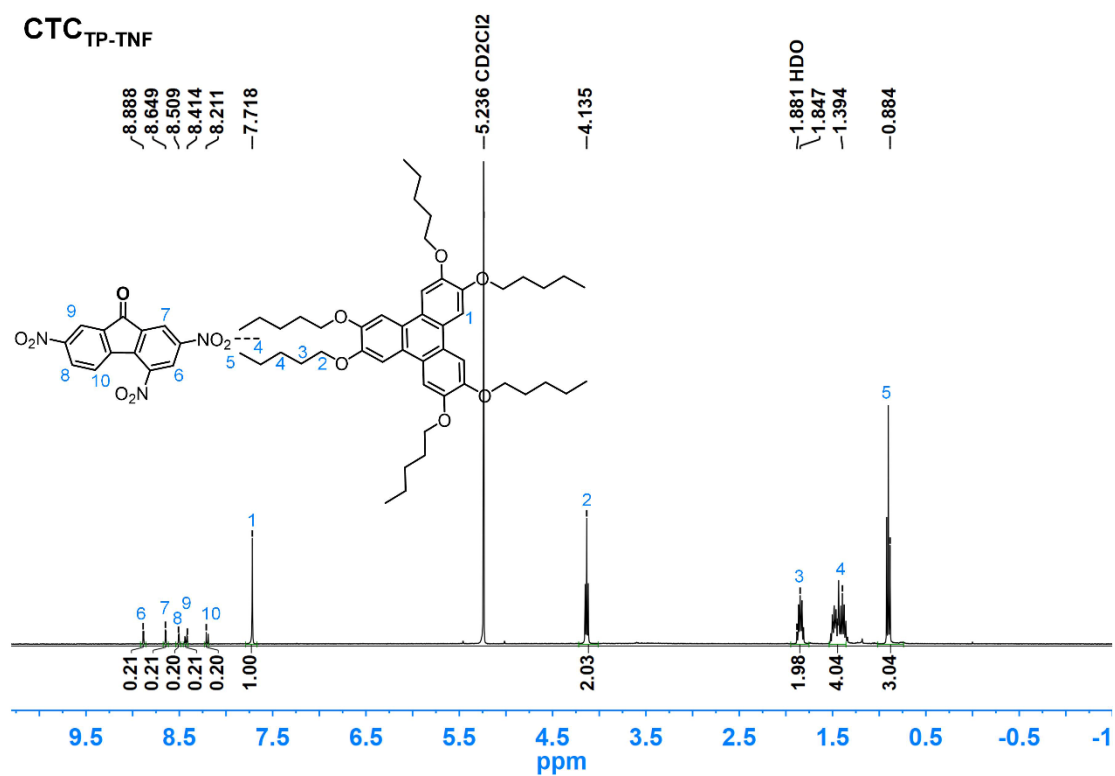


Figure S5. ¹H-NMR spectrum of complex CTC_{TP-TNF}

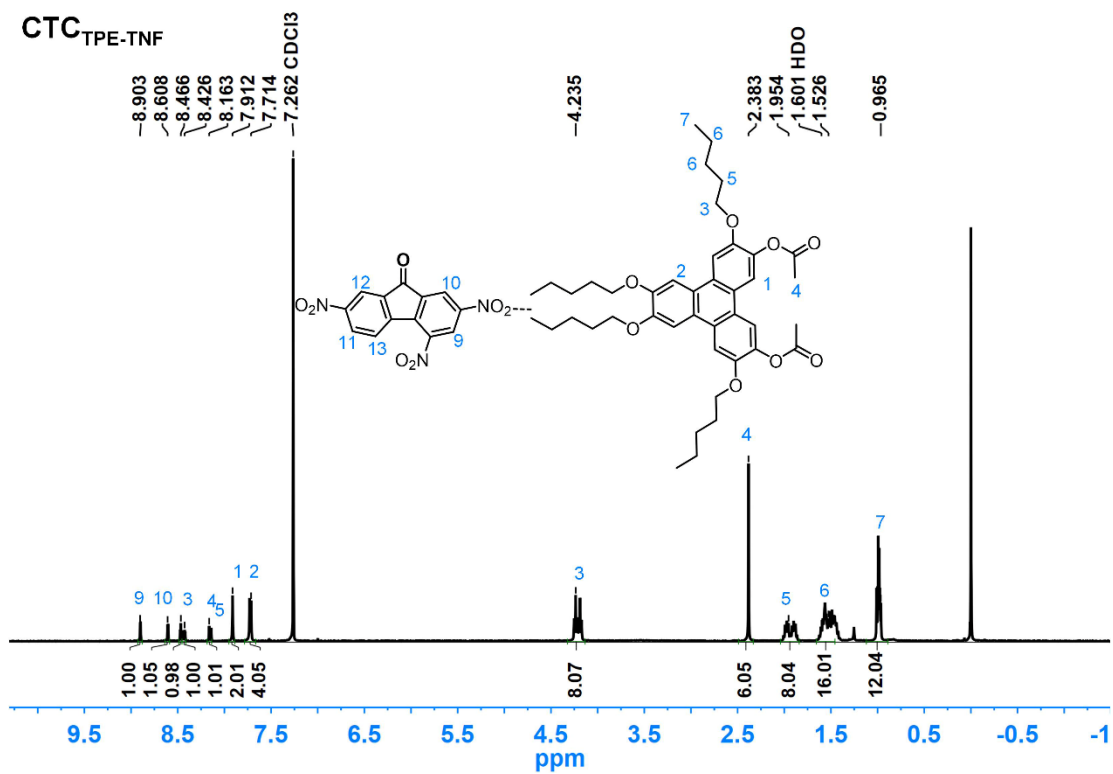


Figure S6. ¹H-NMR spectrum of complex CTC_{TPE-TNF}

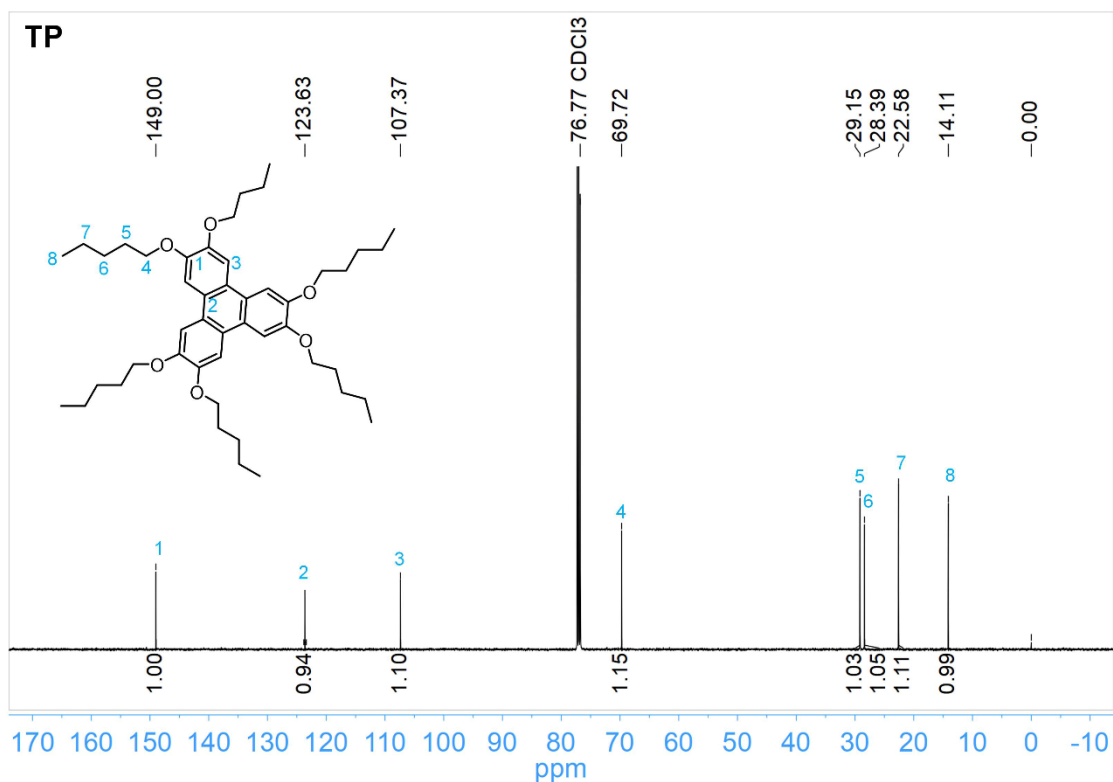


Figure S7. ¹³C-NMR spectrum of compound TP

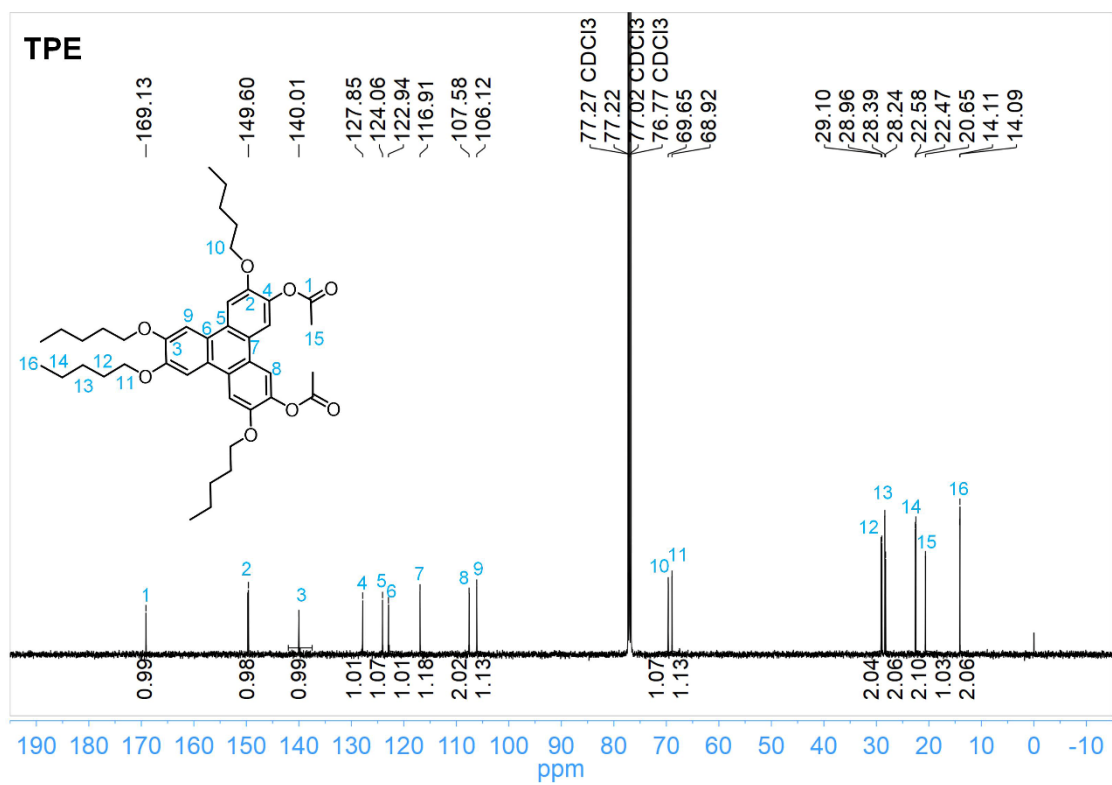


Figure S8. ^{13}C -NMR spectrum of compound TPE

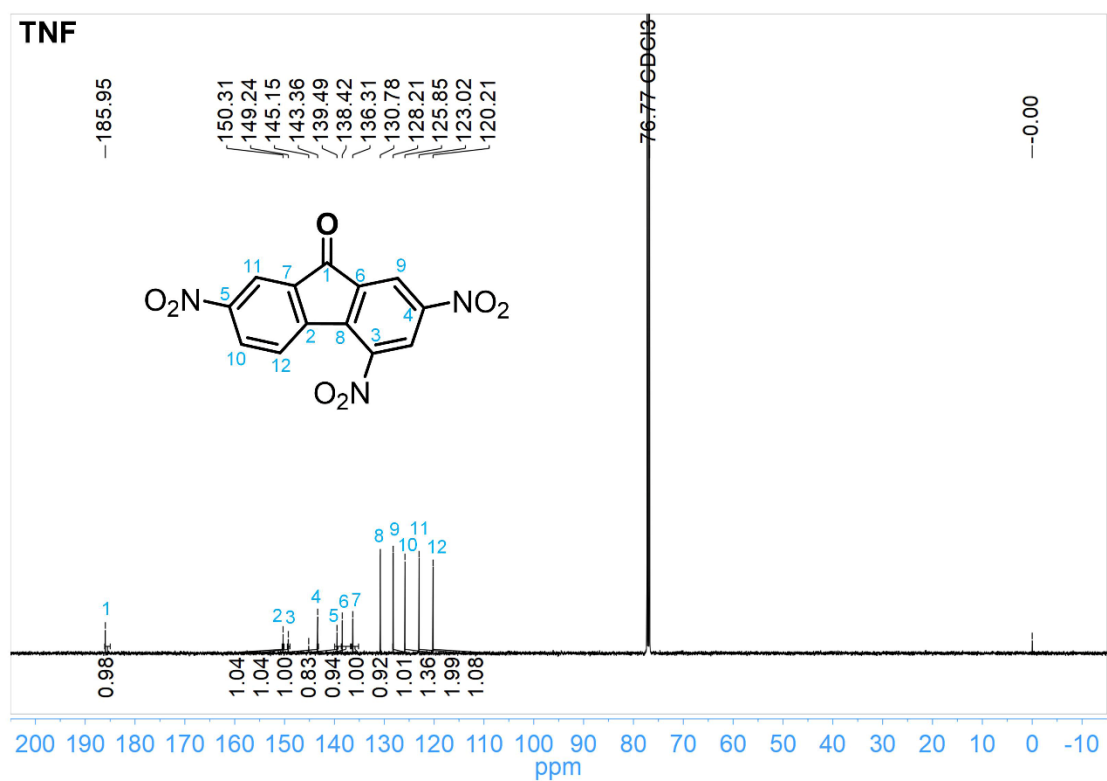


Figure S9. ^{13}C -NMR spectrum of compound TNF

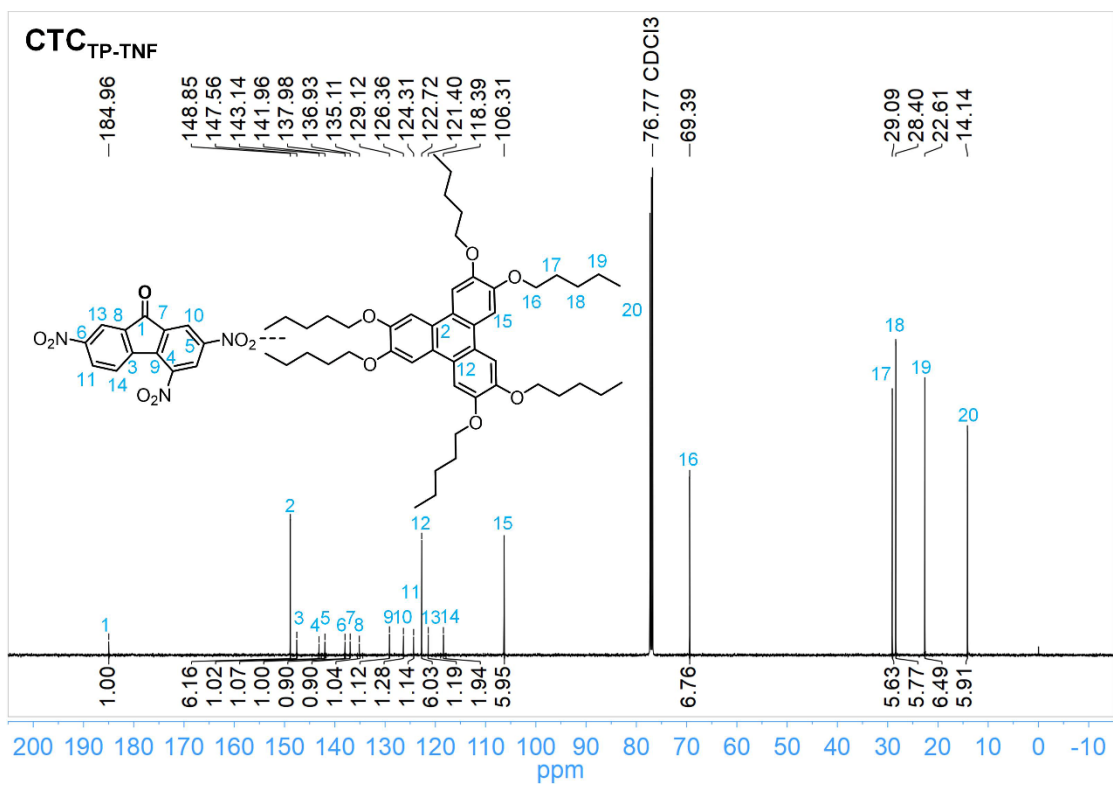


Figure S10. ¹³C-NMR spectrum of compound CTC_{TP-TNF}

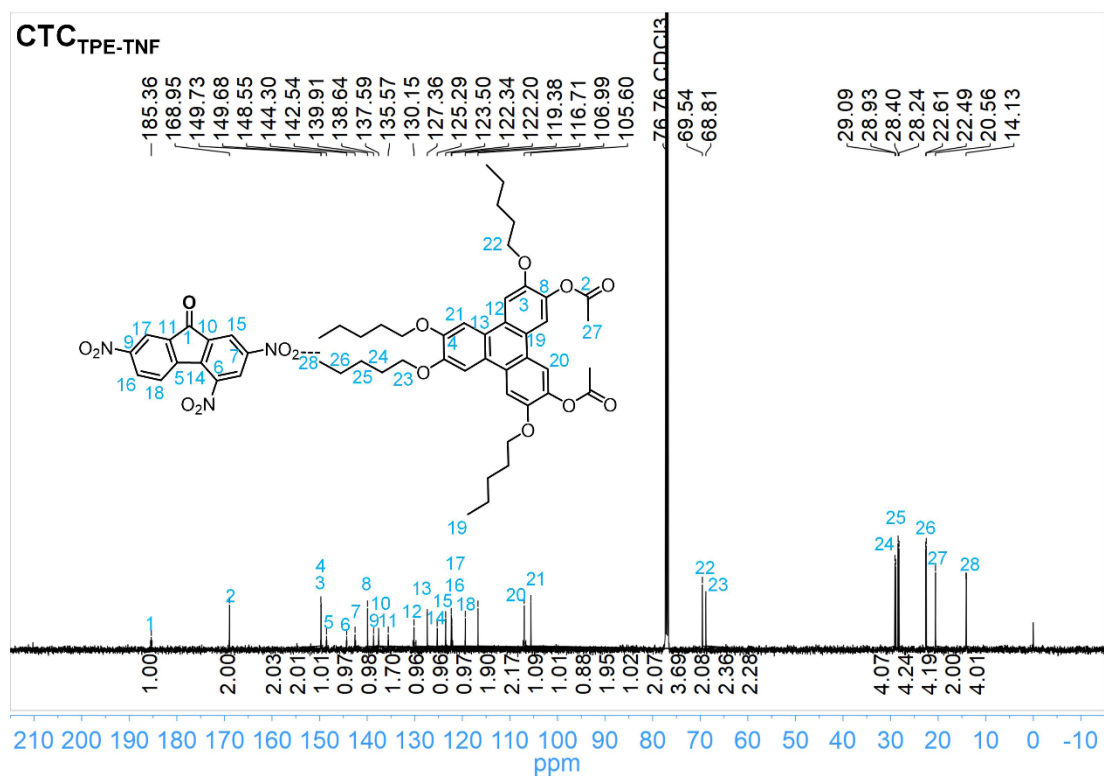


Figure S11. ¹³C-NMR spectrum of compound CTC_{TPE-TNF}

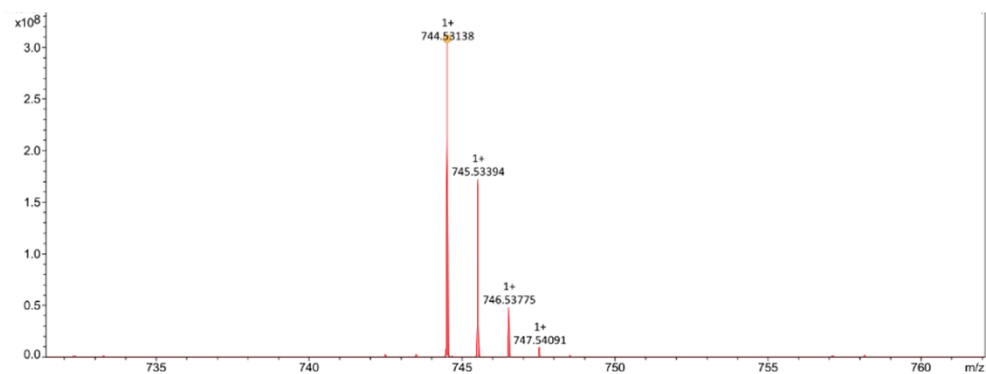


Figure S12. MALDI-TOF mass spectra of compound TP

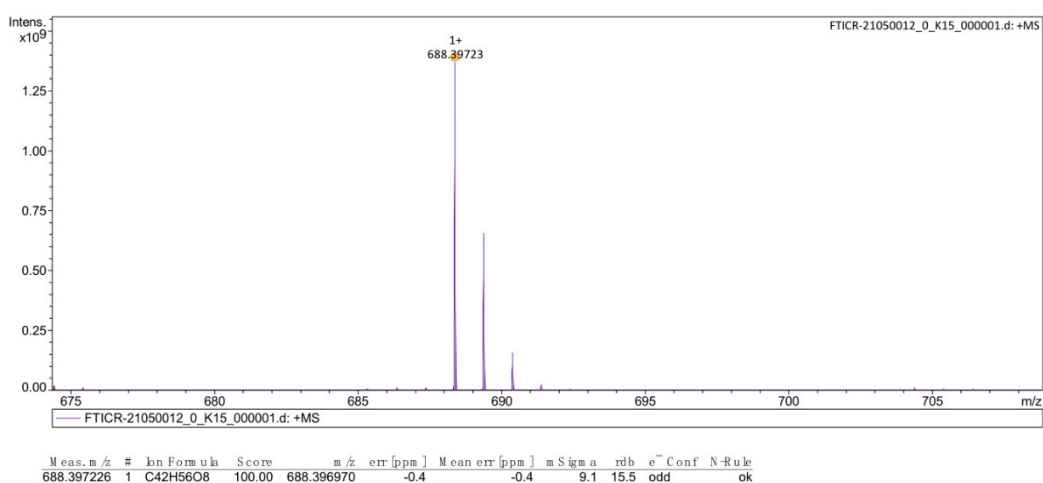


Figure S13. MALDI-TOF mass spectra of compound TPE

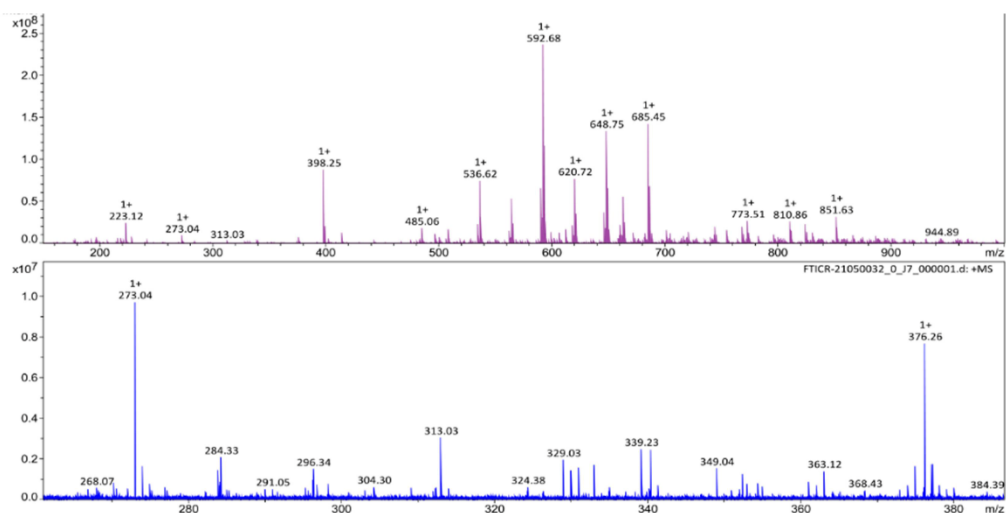


Figure S14. MALDI-TOF mass spectra of compound TNF

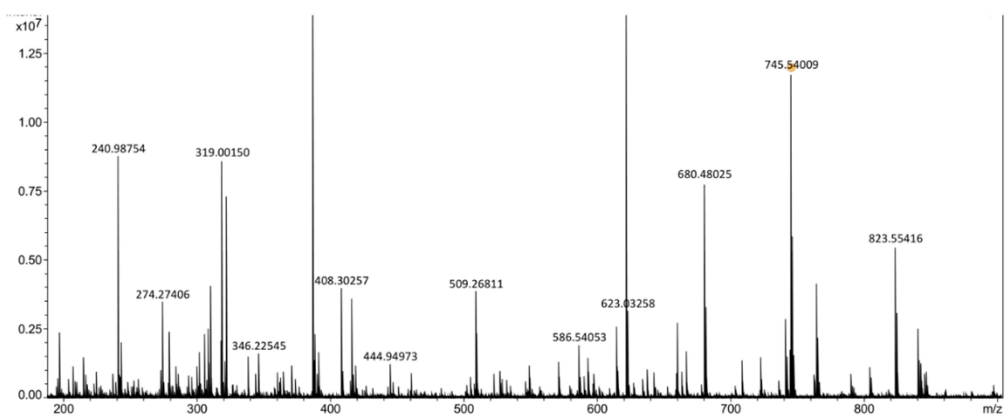


Figure S15. ESI mass spectrum of complex CTC_{TP-TNF}

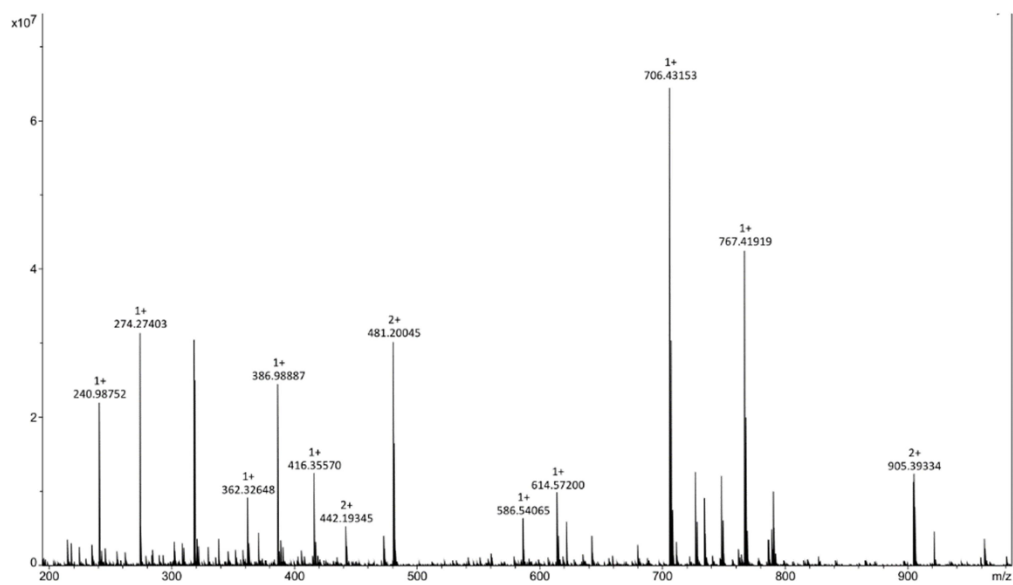


Figure S16. ESI mass spectrum of complex CTC_{TPE-TNF}

Table S3. Summary of FT-IR spectra of compounds.

Sample	Bond	Frequency (cm ⁻¹)				
		C=O	NO ₂	NO ₂	C-O-C	C-O-C
TP		—	—	—	1262	1055
TPE		1751	—	—	1267	1052
TNF		1735	1525	1345	—	—
CTC_{TP-TNF}		1731	1507	1341	1263	1035
CTC_{TPE-TNF}		1730	1508	1342	1265	1049

Table S4. Summary of Raman spectra of compounds

Sample	Bond	Frequency (cm ⁻¹)		
		C=C	C=O	C-NO ₂
TP		1614	—	—
TPE		1614	—	—
TNF		1606	1737	1362
CTC_{TP-TNF}		1605	—	1357
CTC_{TPE-TNF}		1601	1735	1381

3. TGA, DSC, Temperature-dependent FT-IR spectra, POM diagrams, 1D WAXD, 2DXRD patterns

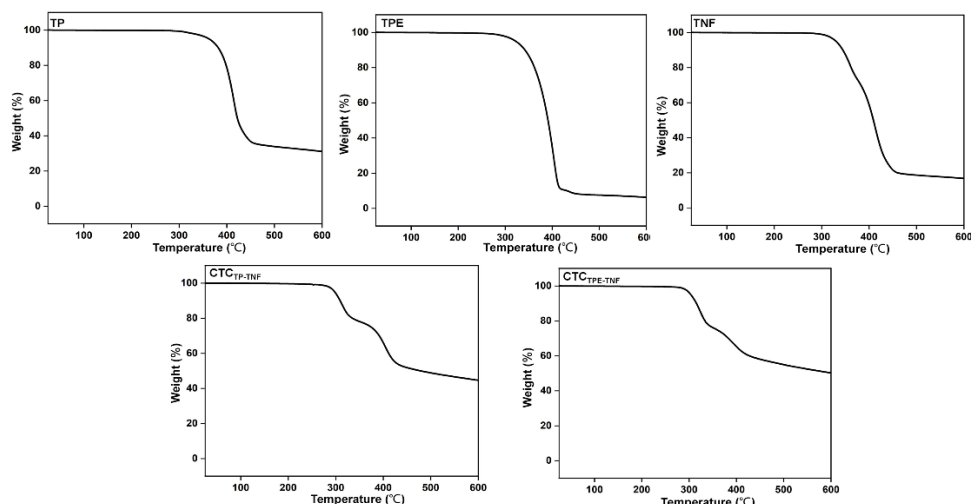


Figure S17. TGA of all molecules and Charge transfer complexes

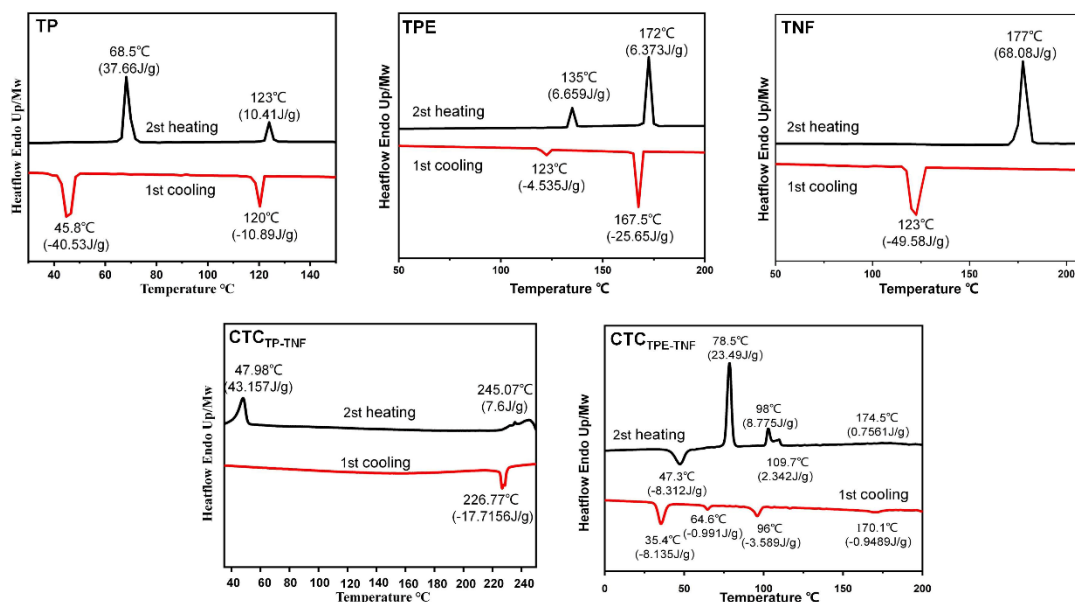


Figure S18. DSC of all molecules

Table S5. Summary of DSC results of all molecules and Charge transfer complexes

sample	2nd heating	1st cooling
TP	Cr _h 68.5°C (37.66J/g) Col _h 123°C (10.41J/g) Iso	Iso 120°C (-10.89J/g) Col _h 45.8°C (-40.53J/g) Cr
TPE	Col _{h1} 135°C (6.659J/g) Col _{h2} 172°C (6.373J/g) Iso	Iso 167.5°C (-25.65J/g) Col _{h2} 123°C (-4.53J/g) Col _{h1}
TNF	Cr177°C (68.08J/g) Iso	Iso 123°C (-49.58J/g) Cr
CTC_{TP-TNF}	Cr47.98°C (43.157J/g) Col _h (245.07J/g) Iso	Iso 226.77°C (-17.715) Col _h
	BCC 47.3°C (-8.312J/g) BCC	
CTC_{TPE-TNF}	78.5°C (23.49J/g) A15 98°C (8.775J/g)	Iso170.1°C (-0.948J/g) A15 104°C A15+Col _h 96°C (-3.589J/g) A15+Col _h 64.6°C (-0.991J/g) A15+Col _h
	DG109.7°C (2.343J/g)	47.3°C (-8.312J/g) A15+Col _h
	BCC174.5°C (0.7561J/g) Iso	

Iso= isotropic phase; Col_h = hexagonal columnar phase; A15= Frank–Kasper A15 phase; BCC= body-centered cubic; DG=double-gyroid phase; Cr=crystalline phase.

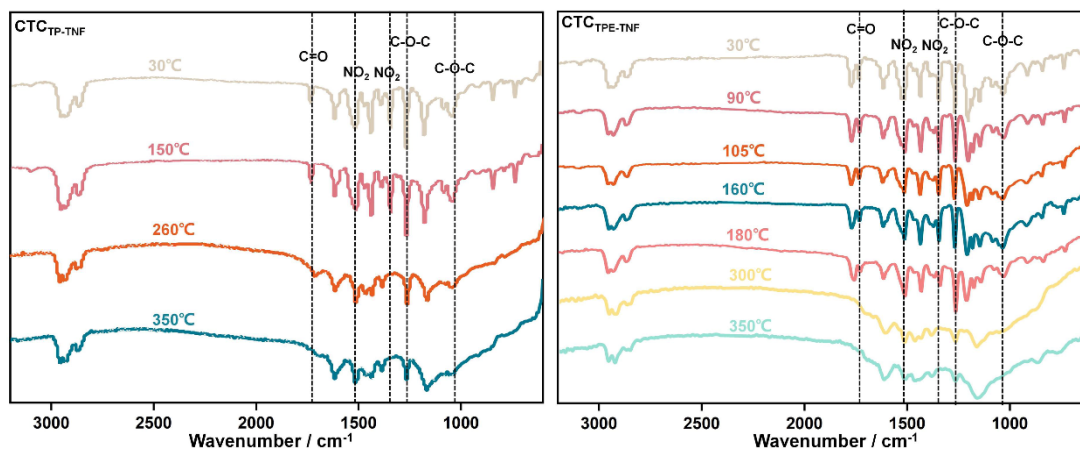


Figure S19. Temperature-dependent FT-IR spectra CTCs

The stability of the charge-transfer interaction was demonstrated by the temperature-dependent FT-IR spectroscopy study. As shown in Fig. S18, the intensities of C=O and NO₂ bands decreased and were accompanied by larger chemical shifts when the temperature was reached the melting temperature. This proved that CTCs were stable over the previous temperature range.

Table S6. Summary of Temperature-dependent FTIR spectra of CTC_{TP-TNF}

Temperature	Bond	Frequency (cm ⁻¹)				
		C=O	NO ₂	NO ₂	C-O-C	C-O-C
30°C		1731	1509	1339	1266	1035
150°C		1734	1504	1338	1264	1033
260°C		1709	1508	-	1261	1039
350°C		1702	1511	-	1260	1039

Table S7. Summary of Temperature-dependent FTIR spectra of CTC_{TPE-TNF}

Temperature	Bond	Frequency (cm ⁻¹)				
		C=O	NO ₂	NO ₂	C-O-C	C-O-C
30°C		1730	1510	1342	1268	1031
90°C		1731	1509	1342	1267	1033
105°C		1731	1506	1340	1265	1032
160°C		1727	1507	1342	1265	1033
180°C		1728	1511	1344	1268	1032
300°C		-	1514	-	1269	-

Thermal properties and phase behaviors of TP and TPE

TP showed two endothermic peaks at 68.5°C (37.66J/g) and 123°C (10.41J/g) during the second heating and two exothermic peaks at 120°C(-10.41J/g) and 45.8°C (-40.53J/g) during the first cooling. Nevertheless, TPE as well as showed two endothermic peaks at 135°C (6.659J/g) and 172°C (6.373J/g) during the heating, two exothermic peaks at 167.5°C (-25.65J/g) and 123°C (-4.535J/g) during the first cooling. TP and TPE (Fig. 13 a-f) observed by POM showed a focal conic fan texture, which was recognized as the classical hexagonal columnar phase (Col_h) phase. The difference was that TP eventually crystallizes at 45.8°C, while 36TPE retains the same liquid crystal texture at room temperature. 1D WAXD data of TP and TPE were obtained during the first cooling. For TP, at 115°C, the diffraction peaks in the range of 2θ = 5-20° can be indexed to (100), (200), (210) with the reciprocal 1/d-spacing ratios 1: √4: √7 which were attributed to hexagonal packing. At 40°C, the 1D WAXD data showed crystalline characteristics. 1D WAXD patterns of TPE obtained at 160°C, 126°C and 40°C showed sharp diffraction peaks in the range of 2θ = 5-20°, indexed as (100), (200), (210), (300), (310) with the reciprocal 1/d-spacing ratios 1: √4: √7: √9: √13 which were confirmed to hexagonal packing. The acceptor molecule (TNF) showed crystal characteristics, with an endothermic peak at 177°C (68.08 J/g) during heating and an exothermic peak at 123°C (-49.58 J/g) during cooling.

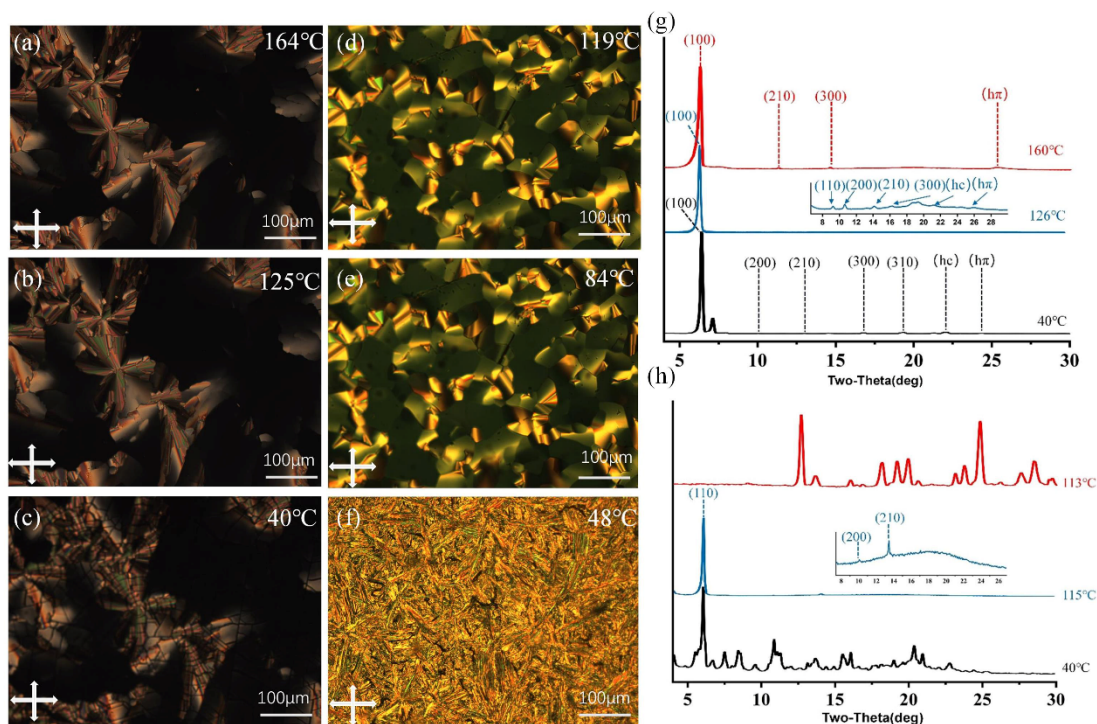


Figure S20. (a), (b) and (c) POM images of TPE; (d), (e) and (f) POM images of TP; (g) 1D WAXD pattern of TPE; (h) 1D WAXD pattern of TP.

Table S8. Summary and detailed indexation of the complementary 1D WAXD data for the individual components

Sample	$d_{\text{obs}}(\text{\AA})^a$	$I[\%]^b$	hkl^c	$d_{\text{cal}}(\text{\AA})^d$	Lattice parameters ^e
TP(40°C)	17.40	vs	100	17.40	Col_h ($a=20.09\text{\AA}$)
$\text{Col}_h/p6mm$	10.09	m	110	10.04	
	8.76	m	200	8.90	
	6.43	m	210	6.57	
	5.71	m	300	5.79	
	4.89	m	310	4.82	
	4.52	w	hc		
	3.53	w	$h\pi$		
TP(115°C)	17.23	vs	100	17.230	Col_h ($a=19.90\text{\AA}$)
$\text{Col}_h/p6mm$	8.75	vw	200	8.62	
	6.57	w	210	6.51	
TPE(40°C)	16.36	vs	100	16.36	Col_h ($a=18.89\text{\AA}$)
$\text{Col}_h/p6mm$	8.24	m	200	8.18	
	6.39	m	210	6.18	
	5.46	m	300	5.45	
	4.67	m	310	4.54	
	4.23	m	hc		
	3.67	w	$h\pi$		

TPE(126°C)	16.56	vs	100	16.56	Col _h (a=19.13Å)
Col _h /p6mmm	9.53	vw	110	9.56	
	8.34	vw	200	8.28	
	6.27	vw	210	6.26	
	5.45	vw	300	5.52	
	4.58	vw	hc	4.59	
	3.42	vw	hπ		
TPE(160°C)	16.61	vs	100	16.61	Col _h (a=19.18Å)
Col _h /p6mmm	6.33	w	210	6.28	
	5.58	w	300	5.54	
	3.52	m	hπ		

$d_{\text{obs}}(\text{Å})^{\text{a}}$: experimentally measured spacings. $I[\%]^{\text{b}}$: intensity of the reflection(vs: very strong, s: strong, m: medium, w: weak, vw: very weak). hkl^{c} : miller indices of the reflection. $d_{\text{cal}}(\text{Å})^{\text{d}}$ and Lattice parameters^e a: deduced from the following mathematical expression; $d_{hkl}=1/(4(h^2+k^2+hk)/(3a)^2)^{1/2}$ for the indexing Col_h lattices.

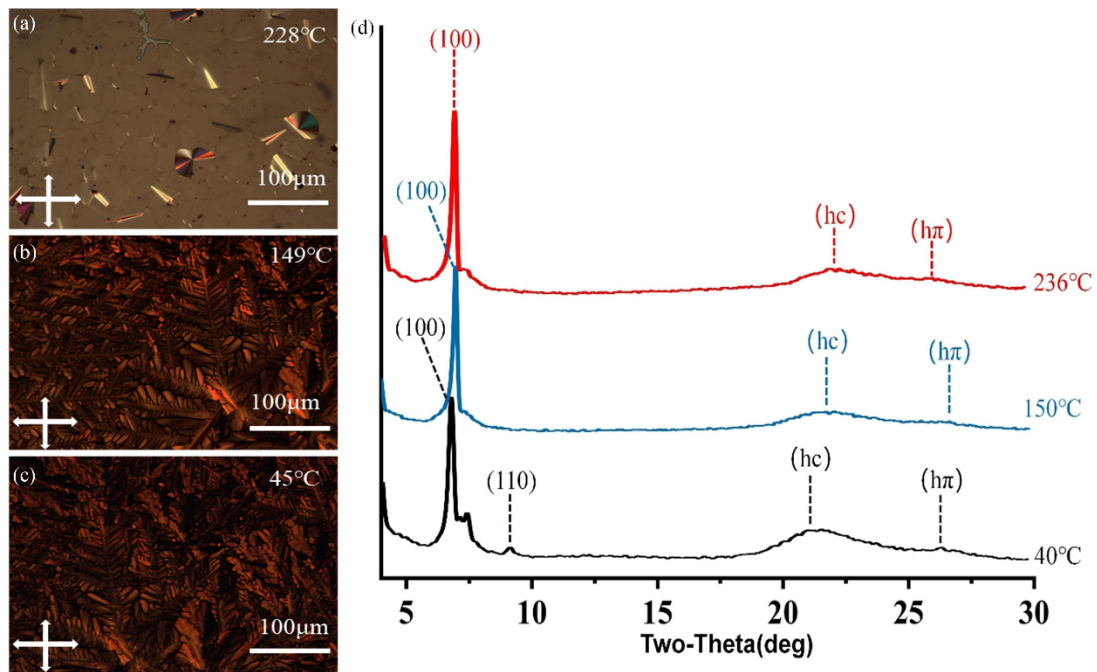


Figure S21. POM images and 1D WAXD pattern of CTC_{TP-TNF}.

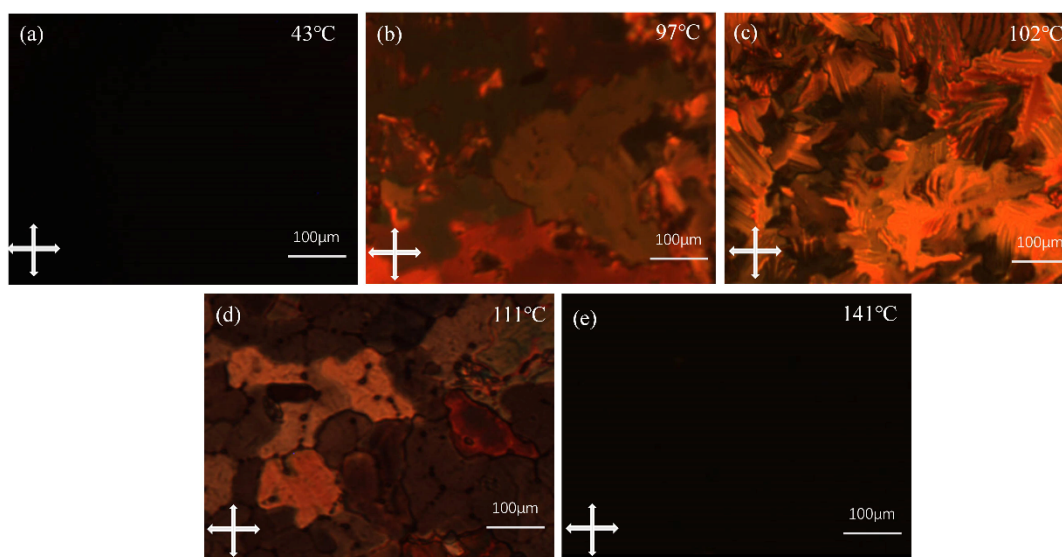


Figure S22. POM images of $\text{CTC}_{\text{TPE-TNF}}$ during the heating.

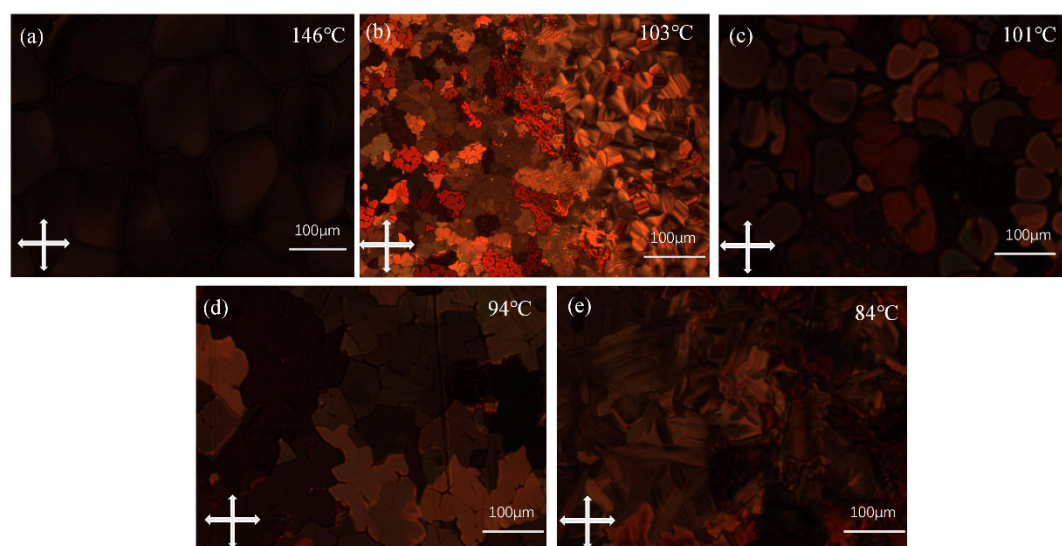


Figure S23. POM images of $\text{CTC}_{\text{TPE-TNF}}$ during the cooling.

Table S9. Summary and detailed indexation of the complementary 1D WAXD data for the CTCs

Sample	$d_{\text{obs}}(\text{\AA})^a$	$I[\%]^b$	hkl^c	$d_{\text{cal}}(\text{\AA})^d$	Lattice parameters ^e
$\text{CTC}_{\text{TP-TNF}} (40^\circ\text{C})$	14.98	vs	100	14.98	Col_h ($a=17.31\text{\AA}$)
	10.52	m	110	10.59	$D=17.31\text{\AA}$
	4.17	s	hc		$\mu=1$
$\text{CTC}_{\text{TP-TNF}} ((150^\circ\text{C}))$	3.37	m	$h\pi$		
	14.50	vs	100	14.49	Col_h ($a=16.73\text{\AA}$)
	4.22	s	$h\pi$		$D=16.31\text{\AA}$
	4.06	m	$h\pi$		$\mu=1$

CTC _{TP-TNF} (236°C)	14.77	vs	100	14.77	Col _h (a=17.06Å)
Col _h /p6mmm	4.06	s	hc		D=17.06Å
	4.00	m	hπ		μ=1
CTC _{TPE-TNF} (25°C)	22.30	m	110	22.30	A15(a=31.53Å)
A15/ <i>pm</i> ₃ ⁻ <i>n</i>	12.40	m	211	12.87	D=19.86Å
	11.16	m	220	11.15	μ=3
	10.62	m	310	9.80	
	7.99	m	400	7.88	
	7.46	w	411	7.43	
	6.93	w	421	6.88	
	6.51	w	422	6.40	
	6.18	w	510	6.18	
BCC/ <i>Im</i> ₃ ⁻ <i>m</i>	13.558	s	110	13.55	BCC(a=19.16Å)
	9.348	s	200	9.58	D=18.87Å
	6.01	s	310	6.06	μ=2
	5.09	m	321	5.12	
	4.90	m	400	4.78	
Col _h /p6mmm	16.67	m	100	16.67	Col _h (a=19.25Å)
	9.74	s	110	9.60	D=19.25Å
	5.63	m	300	5.56	μ=1
	4.25	m	hc		
	3.35	m	hπ		
	3.32	m	hπ		
CTC _{TPE-TNF} (75°C)	22.48	m	110	22.48	A15 (a=31.79Å)
A15/ <i>pm</i> ₃ ⁻ <i>n</i>	12.45	m	211	12.97	D=19.72Å
	11.27	m	220	11.24	μ=3
	8.03	w	400	7.94	
	7.53	w	411	7.49	
	6.96	w	421	6.94	
	6.67	w	332	6.78	
	6.22	w	510	6.23	
BCC/ <i>Im</i> ₃ ⁻ <i>m</i>	13.62	s	110	13.62	BCC (a=19.26Å)
	6.06	m	310	6.10	D=18.96Å
	5.13	w	321	5.10	μ=2
	4.92	w	400	4.81	
Col _h /p6mmm	16.94	m	100	16.94	Col _h (a=19.56Å)
	9.83	m	110	9.78	D=19.56Å
	5.64	m	300	5.65	μ=1
	4.75	m	310	4.70	
	4.27		hc		
	3.37	m	hπ		
	3.34	m	hπ		
CTC _{TPE-TNF} (90°C)	22.04	m	110	22.58	A15 (a=31.93Å)

$A15/pm\bar{3}n$	15.50	s	200	15.96	D=19.8Å	
	14.28	s	210	14.29	$\mu=3$	
	13.18	s	211	13.03		
	10.94	m	310	10.10		
	7.93	w	400	7.53		
	7.56	m	411	7.53		
	7.11	m	420	7.14		
	6.23	w	510	6.26		
$Col_h/p6mmm$	6.06	w	520	5.93		
	16.99	m	100	16.99	Col_h (a=19.61Å)	
	9.84	w	110	9.80	D=19.61Å	
	6.473	w	210	6.42	$\mu=1$	
	5.50	w	300	5.66		
	3.42	m	$h\pi$			
$CTC_{TPE-TNF} (108^\circ C)$	3.33	m	$h\pi$			
	15.41	s	211	15.41	DG (a=37.74Å)	
	$DG/1a\bar{3}d$	13.18	s	220	13.34	
		9.31	m	400	9.43	
		7.56	m	431	7.40	
		6.60	m	440	6.67	
5.86		w	541	5.82		
$A15/pm\bar{3}n$	10.99	m	220	11.00	A15 (a=31.08Å)	
	9.85	m	310	9.88	D=19.28Å	
	6.35	m	422	6.37	$\mu=3$	
	6.23	m	430	6.25		
	5.50	w	440	5.52		
	3.53	m	$h\pi$			
	3.49	m	$h\pi$			
	$CTC_{TPE-TNF} (165^\circ C)$	13.77	s	110	13.77	BCC (a=19.26Å)
$BCC/1m\bar{3}m$		3.54	m	$h\pi$	D=18.97Å	
		3.51	m	$h\pi$	$\mu=2$	
$CTC_{TPE-TNF} (104^\circ C)$	15.17	s	200	15.9	A15 (a=30.33Å)	
	$A15/pm\bar{3}n$	14.29	s	210	14.28	D=18.81Å
		13.62	s	211	13.00	$\mu=3$
		10.23	m	310	10.10	
		6.63	m	422	6.52	
		5.56	w	440	5.65	
		4.40	m	hc		
		3.51	m	$h\pi$		
		3.40	m	$h\pi$		
$CTC_{TPE-TNF} (89^\circ C)$	15.27	s	200	15.90	A15 (a=30.54Å)	
	$A15/pm\bar{3}n$	14.25	s	210	14.25	D=18.95Å
		10.05	s	310	10.07	$\mu=3$
		6.62	m	421	6.66	

Col _h /p6mmm	16.99	m	100	16.99	Col _h (a=19.62Å)	
	6.50	w	210	6.40	D=19.62Å	
	5.56	w	300	5.66	μ=1	
	4.09	m	hc			
	3.48	m	hπ			
	3.40	m	hπ			
CTC _{TPE-TNF} (41°C) A15/p $\bar{3}n$	19.78	m	110	19.78	A15 (a=28.41Å)	
	14.21	s	200	14.00	D=17.62Å	
	12.35	s	210	12.50	μ=2	
	10.17	m	220	10.00		
	8.20	m	222	8.10		
	6.65	m	411	6.60		
	5.11	w	521	5.11		
	4.94	w	440	4.94		
	Col _h /p6mmm	16.83	m	100	16.83	Col _h (a=19.43Å)
		9.63	m	110	9.72	D=19.43Å
8.46		m	200	8.42	μ=1	
5.70		w	300	5.61		
4.63		w	310	4.67		
4.43		m	hc			
3.36		m	hπ			
3.33		m	hπ			
CTC _{TPE-TNF} (32°C) A15/p $\bar{3}n$	22.20	m	110	22.20	A15 (a=31.4Å)	
	12.35	m	210	12.80	D=19.48Å	
	11.22	m	220	11.10	μ=3	
	10.66	m	310	10.00		
	8.48	m	321	8.39		
	7.63	w	410	7.61		
	7.47	w	411	7.40		
	6.62	w	332	6.69		
	6.14	w	510	6.15		
	Col _h /p6mmm	16.83	s	100	16.83	Col _h (a=19.43Å)
9.74		m	110	9.71	D=19.43Å	
6.25		m	210	6.35	μ=1	
5.67		w	300	5.61		
4.63		w	310	4.67		
4.43		m	hc			
3.35		m	hπ			
3.32		m	hπ			

d_{obs}(Å)^a: experimentally measured spacings. I[%]^b: intensity of the reflection (vs: very strong, s: strong, m: medium, w: weak, vw: very weak). hkl^c: miller indices of the reflection. d_{cal}(Å)^d and Lattice parameters^e $a = 2\sqrt{3}/3 \cdot d \cdot \sqrt{h^2 + k^2 + hk}$, $D_{col} = a$;

$\mu = \sqrt{3}/2 \cdot (N_A \rho a^2 t / M_{wt})$ for the indexing Col_h lattices; $a = d_{100}; D = 2\sqrt[3]{3a^3}/8\pi$;
 $\mu = 1/2 \cdot (N_A \rho a^3 / M_{wt})$ for the indexing BCC lattices;
 $a = \sqrt{4}d_{200} + \sqrt{5}d_{210} + \sqrt{6}d_{211}/3$; $D = 2\sqrt[3]{3a^3}/32\pi$; $\mu = 1/8 \cdot (N_A \rho a^3 / M_{wt})$ for
 the indexing A15 lattices. (Where N_A is Avogadro's number ($6.022 \times 10^{23} \text{ mol}^{-1}$), ρ is
 the experimental density. (ca. $1. \pm 0.2 \text{ g/cm}^3$), M_{wt} is the theoretical average molecular
 weight, t is the distance between π - π .

4. Self-assembly behavior of CTCs

Table S10. dipole moments of all molecular

Sample	Dipomoment (Total)	Dipomoment (X)	Dipomoment (Y)	Dipomoment (Z)
TP	0.00	0.00	0.00	0.00
TPE	2.65	0.00	2.65	0.00
TNF	1.27	-0.22	1.18	-0.42
CTC _{TP-TNF}	2.13	0.90	1.79	0.74
CTC _{TPE-TNF}	4.61	3.11	0.88	-3.28

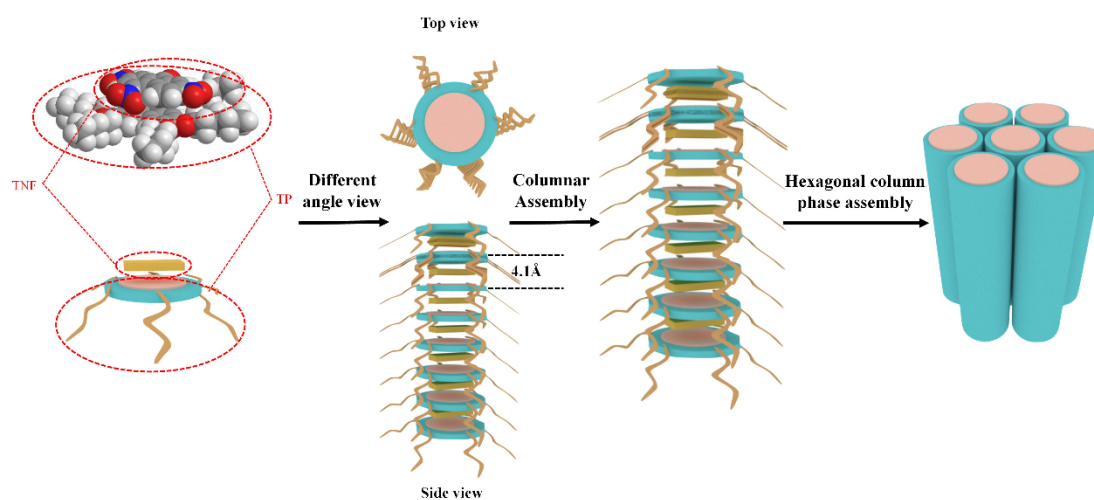


Figure S24. Schematic diagram of the CTC_{TP-TNF} hierarchical self-assembly mechanism

5 TOF: Mobility of CTC_{TPE-TNF} as a function of temperature and double logarithmic plots of typical transient current

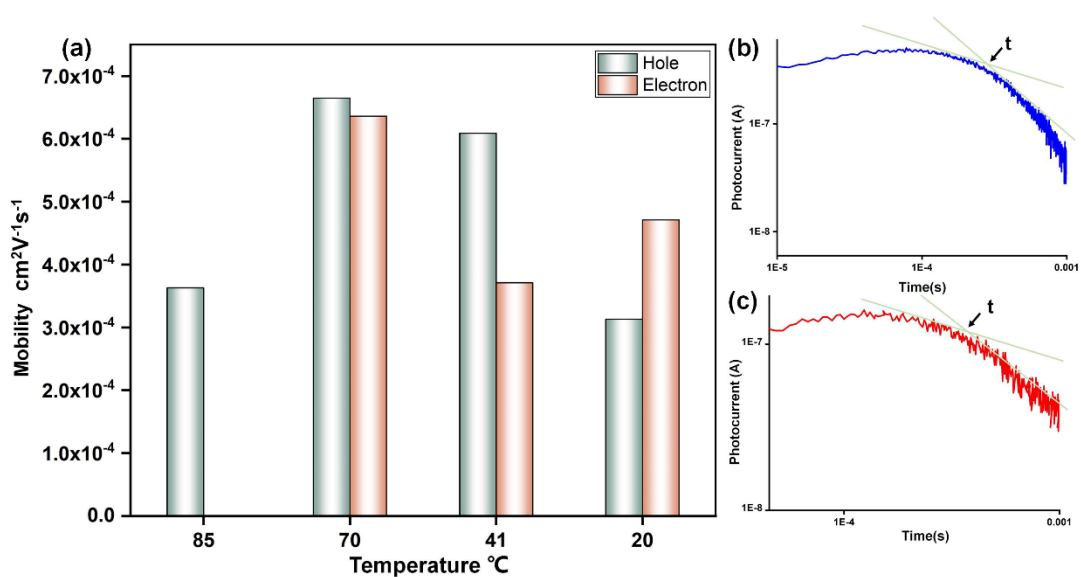


Figure S25. (a) Mobility of CTC_{TPE-TNF} as a function of temperature from 90°C to 20 °C; Double logarithmic plots of typical transient current I as a function of time t of CTC_{TPE-TNF} in an electric field of $E = 2.2 \times 10^4 \text{ Vcm}^{-1}$ (c) hole mobility of CTC_{TPE-TNF}: $\mu_h = 3.13 \times 10^{-4} \text{ cm}^2\text{V}^{-1}\text{s}^{-1}$; b) electron mobility of CTC_{TPE-TNF}: $\mu_e = 3.71 \times 10^{-4} \text{ cm}^2\text{V}^{-1}\text{s}^{-1}$.